Oecologia (2002) 133:295–306
DOI 10.1007/s00442-002-1019-0

ECOPHYSIOLOGY

Kristin Palmqvist · Lena Dahlman
Fernando Valladares · Anders Tehler
Leopoldo G. Sancho · Jan-Eric Mattsson

CO_2 exchange and thallus nitrogen across 75 contrasting lichen associations from different climate zones

Received: 22 December 2001 / Accepted: 27 June 2002 / Published online: 5 September 2002

Abstract Aiming to investigate whether a carbon-to-nitrogen equilibrium model describes resource allocation in lichens, net photosynthesis (NP), respiration (*R*), concentrations of nitrogen (N), chlorophyll (Chl), chitin and ergosterol were investigated in 75 different lichen associations collected in Antarctica, Arctic Canada, boreal Sweden, and temperate/subtropical forests of Tenerife, South Africa and Japan. The lichens had various morphologies and represented seven photobiont and 41 mycobiont genera. Chl *a*, chitin and ergosterol were used as indirect markers of photobiont activity, fungal biomass and fungal respiration, respectively. The lichens were divided into three groups according to photobiont: (1) species with green algae, (2) species with cyanobacteria, and (3) tripartite species with green algal photobionts and cyanobacteria in cephalodia. Across species, thallus N concentration ranged from 1 to 50 mg g^{-1} dry wt., NP varied 50-fold, and R 10-fold. In average, green algal lichens had the lowest, cyanobacterial *Nostoc* lichens the highest and tripartite lichens intermediate N concentrations. All three markers increased with thallus N concentration, and lichens with the highest Chl *a* and N concentrations had the highest rates of both P and R. Chl *a* alone accounted for ca. 30% of variation in NP and R across species. On average, the photosynthetic efficiency quotient [K_F=(NP_{max}+R)/R)] ranged from 2.4 to 8.6, being higher in fruticose green algal lichens than in foliose *Nostoc* lichens. The former group invested more N in Chl *a* and this trait increased NP_{max} while decreasing R. In general terms, the investigated lichens invested N resources such that their maximal C input capacity matched their respiratory C demand around a similar (positive) equilibrium across species. However, it is not clear how this apparent optimisation of resource use is regulated in these symbiotic organisms.

Keywords Photosynthesis · Resource allocation · Respiration · Symbiosis · Lichen

K. Palmqvist (✉) · L. Dahlman
Department of Ecology and Environmental Science,
Umeå University, 901 87 Umeå, Sweden
e-mail: kristin.palmqvist@eg.umu.se
Tel.: +46-90-7869184, Fax: +46-90-7866705

F. Valladares
Centro de Ciencias Medioambientales,
CSIC. Serrano 115 dpdo. 28006 Madrid, Spain

A. Tehler
Naturhistoriska riksmuseet, Sektionen för kryptogambotanik,
Box 50007, 104 05, Stockholm, Sweden

L.G. Sancho
Departamento de Biología Vegetal II, Facultad de Farmacia,
Universidad Complutense 28040 Madrid, Spain

J.-E. Mattsson
Lövlundsvägen 3, 743 34 Storvreta, Sweden

Introduction

Lichens are nature's pioneers living in almost all terrestrial habitats and being particularly important in the most barren and inhospitable parts of the world (Kappen 1988). The lichen partners of fungus (mycobiont) plus alga and/or cyanobacterium (photobiont) form a thallus that appears as a new and integrated organism. However, lichens can be regarded as a fungal nutritional strategy (Honegger 1996a) and are placed taxonomically among other fungi (Eriksson and Winka 1998). This life-style has evolved several times (Gargas et al. 1995) and there is a high degree of genetic diversity among the ca. 13,500 lichen-forming fungi (Honegger 1996a, b; Tehler 1996). In addition, around 100 algal and cyanobacterial genera have been recorded from lichens (Tschermak-Woess 1988).

Being poikilohydric organisms, the carbon budget of lichens is passively controlled by the environment, with photosynthetic activity limited by water and light availability, and respiration controlled by water and temperature (Kershaw 1985; Palmqvist 2000; Lange et al. 2001). Transport and distribution of photosynthetic products from photo- to mycobiont may also be environmentally controlled, being dependent on repeated drying and wetting of the thallus (Kershaw 1985). Despite this strong

environmental influence on their carbon budget, lichens must still be able to maintain a positive energy balance in order to grow and survive. The photobiont provides the carbon, but we know little about the energy demand of either the mycobiont or the photobiont (Kershaw 1985; Palmqvist 2000). In addition to carbon, the lichen must also acquire mineral nutrients, such as nitrogen, that are generally acquired passively through wet or dry deposition (Nash 1996), the exception being ca. 1300 species with cyanobacterial photobionts that fix N_2 (Rai 1988; Tschermak-Woess 1988).

In all photoautotrophic organisms, carbon and nitrogen economies are tightly coupled where nitrogen investments in carbon-acquiring shoots must be balanced in relation to mineral-acquiring but carbon-expending roots (Chapin et al. 1987). For lichens, there is a similar trade-off between nitrogen investment into carbon-acquiring photobiont cells on the one hand and carbon-expending mycobiont structures on the other. In addition, the dominant non-photosynthetic fungus has not only basic nitrogen requirements for proteins, nucleic acids etc., but also an additional nitrogen requirement for fungal cell wall (chitin) synthesis. These expenditures are still inevitable, because mycobiont growth is required for increasing thallus area, increasing both potential light interception and mineral acquisition. According to functional equilibrium models (Brouwer 1962), it is assumed that acquired resources are allocated to different structures so that pool sizes of key elements remain constant within and between organs (Schulze and Chapin 1987), and that environmental limitations or excesses that reduce resource use will also reduce uptake (Chapin 1991). This model has been summarised as: when the C:N ratio of a tissue is too high, grow root; otherwise grow shoot, assuming that each species has a specific optimal C:N ratio (Grace 1997). It was suggested recently that the same model is applicable to lichens by replacing shoot with photobiont and root with fungal hyphae (Palmqvist 2000). However, before discussing the validity of such a generalised model for lichens, we needed to collect data for a broad range of species, as has been done for plants (cf. Enriquez et al. 1996; Reich et al. 1998, 1999). For instance, regulatory systems to optimise resource allocation in the thallus might be more or less developed depending on evolutionary lineage (Gargas et al. 1995; Tehler 1996). Lichens are, moreover, constrained by a requirement for coordinated growth between the partners, so their ability to redirect resource investments in response to altered resource supply may be relatively low (Feige and Jensen 1992; Sundberg et al. 2001; Dahlman et al. 2002). Furthermore, C:N ratio optima may vary depending on photobiont (Palmqvist et al. 1998), thallus morphology, or between populations from contrasting habitats (Sancho et al. 2000). In the present study, 75 lichen associations were selected to cover as broad a spectrum as possible of taxonomy, morphology, habitat, and nitrogen requirements. For these, we measured photosynthetic capacity, steady-state respiration, thallus nitrogen (N) concentration, and concentrations of chlorophyll, chitin and ergosterol, aiming to test whether lichens also fit into a generalised C:N equilibrium model.

Materials and methods

Lichen material

The investigated species and number of samples are listed in Appendix 1. Each sample was a complete thallus, a large lobe or a number of neighbouring lobes, hereafter defined as an individual sample. In general, three samples represented each lichen association. Twelve lichens were collected in more than one biome and were thereby represented by more than 3 samples (Appendix 1). Care was taken to avoid sub-sampling of the same individual by collecting thalli from different locations. Sample sizes ranged from 0.1 to ca. 2 g dry wt. and from 5 to 40 cm^2 across species, varying less within species.

The Antarctic lichens were collected in the vicinity of the Spanish Antarctic Base Juan Carlos I (Livingston Island, South Shetland Islands, Antarctica 62°40′S–60°23′W) in January and February 1997. With the exception of *Evernia prunastri* and N-fertilised *Hypogymnia physodes* (Appendix 1), the boreal lichens were collected in August 1997 from typical substrates and habitats in the county of Västerbotten, Sweden (64 to 66°N and 15 to 21°E). With the exception of one Japanese and two South African species (Appendix 1), the temperate/subtropical lichens were collected on Tenerife (28°N–17°W) in January 1998. The Arctic lichens were collected north of 62°N and between 60 to 140°W during a Tundra North West (TNW 99) expedition in June to August 1999 organised by the Swedish Polar Research Secretariat.

Systematics, grouping of species and outliers

Lichens were identified to the species level following the nomenclature of Purvis et al. (1992). Systematics and classification (Appendix 1) follow Tehler (1996) and Eriksson and Winka (1998). Photobionts were based on literature data (Purvis et al. 1992; Tschermak-Woess 1988) or have been confirmed in our own previous studies. Replicate thalli of all except the Antarctic samples have been catalogued and stored at Umeå University. For the initial analysis, the lichens were divided into three groups according to photobiont: (1) species with green algae, (2) species with cyanobacterial *Nostoc*, and (3) tripartite species with green algal photobionts and cyanobacteria in cephalodia (Appendix 1). *Ephebe lanata* with *Stigonema* photobionts, N-fertilised *H. physodes* and "penguin colony" *Usnea aurantiaco-atra* (Appendix 1) were treated as "outliers" throughout. Apart from these, all the obtained data were included in the different analyses and plots unless stated otherwise in the text.

CO_2 gas exchange

Net photosynthetic (NP) and respiratory (R) CO_2 gas-exchange rates were measured for all samples, except for the Canadian lichens. For the Antarctic lichens, measurements were made in the Spanish Antarctic Base in situ using a minicuvette gas exchange system (CMS400, Heinz-Walz, Germany) and a differential IRGA (Binos 100, Leybold-Haeraeus, Germany). Gas-exchange rates were obtained at 5°C and ambient CO_2 (ca. 350 µl l^{-1}), as detailed in Valladares and Sancho (2000). Thalli were collected fresh and wet from the field and maximum net photosynthesis was measured at light saturation (1700 µmol m^{-2} s^{-1}) and optimal hydration, i.e. the hydration level rendering maximum rates during dehydration. Respiration was measured in darkness until steady-state rates were reached.

After collection, the boreal and temperate/subtropical lichens were slowly dried at 15°C under weak illumination (10 µmol m^{-2}

s^{-1}) and stored thereafter in their dry state at 15°C for up to 3 months. Prior to gas-exchange measurements, samples were rehydrated and re-activated at 15°C and 100% RH for 16–20 h in darkness to allow stabilisation of respiration (Kershaw 1985; Sundberg et al. 1999). CO_2 gas-exchange rates were measured with the type of mini-cuvette/IRGA system described above, using projector lamps as light source, as detailed before (Palmqvist 1993). After re-activation, samples were lightly sprayed with water, gently blotted with tissue paper to remove excess water, and placed in the CO_2 gas exchange system measuring first R then light saturated net photosynthesis (NP_{max}) at 10°C and then R at 10°C again; the cuvette temperature was then increased to 15°C and the R, NP and R cycle repeated. Respiration at 10°C reached steady state within 15–20 min, while NP often required at least 1 h to reach steady state with full induction of all photosynthetic processes. The sample was allowed to dry out somewhat during the 10°C measurement, making it possible to determine NP_{max} at optimal hydration for each thallus. If R had declined after the light period, the two R values were averaged. The increase from 10 to 15°C resulted in an initial CO_2 burst followed by stabilisation of CO_2 efflux rates (Sundberg et al. 1999), but again the steady-state R rate was used in the comparisons. It was sometimes necessary to rehydrate the lichen somewhat to obtain NP_{max} at optimal hydration at 15°C. Irradiance level required for light saturation was determined for separate samples of each species and collection site (see Appendix 1). For lichens with green algal photobionts, it was possible to determine this level using fluorescence yield measurements (PAM-2000, Heinz-Walz Effeltrich, Germany). Due to the peculiarities of cyanobacterial fluorescence patterns (Campbell et al. 1998), fluorescence yield measurements cannot easily be used to determine light-saturating irradiances in cyanolichens (Sundberg et al. 1997). Instead, separate CO_2 gas exchange–light response curves were made to determine light saturation irradiances for these species. Further details of CO_2 gas-exchange equipment, light sources and calculations are given elsewhere (Palmqvist 1993).

Cellular markers

Chlorophyll *a* was used as a marker for the photobiont cells (Raven 1992; Enriquez et al. 1996) and the fungal cell wall component chitin was used to assess fungal biomass as in Palmqvist et al. (1998). Ergosterol is the dominant sterol in most fungi, including lichens (Elix 1996), being the principal constituent of the fungal plasma membrane (Weete 1973). This compound has been correlated positively to steady-state respiration rates in lichens (Sundberg et al. 1999) and used as a marker for the metabolic activity of fungi in mycorrhizal associations with plants (Ekblad and Näsholm 1996).

Preparation for sub-cellular analysis

After the gas-exchange measurements, sample area was determined for foliose lichens when the thallus was wet and fully expanded by making a photocopy, which was then analysed with a leaf-area meter (Li-Cor, Nebraska, USA). All samples except the Antarctic material were freeze-dried and thallus dry weights determined to the nearest 0.1 mg. All samples were then milled to a homogenous powder, subsampled for the different assays, and stored dry in desiccators at –18°C to await analysis. The Antarctic lichens were allowed to desiccate at the campsite and placed in dry paper bags for transportation to Spain for chlorophyll and nitrogen analysis (May 1997). The remaining Antarctic material was stored dry in a freezer (–18°C) before ergosterol and chitin analysis in Sweden (April 1999). However, at this stage, no ergosterol was detected due to its degradation during the prolonged storage, while there was no evidence of chitin degradation in the Antarctic material. The Arctic material was dried in darkness at 20°C on board the expedition ship, placed in dry paper boxes, and posted to Sweden within 3–4 weeks after collection. Upon arrival in Sweden, these lichens were sprayed with water, rinsed from debris and immediately freeze-dried, homogenised and analysed. This latter procedure minimised ergosterol degradation (Dahlman et al. 2001). Apart from the rinsing with water prior to gas-exchange measurements or freeze-drying, thalli were not further cleaned before subcellular analysis.

Chlorophyll analysis

Chlorophyll was quantified spectrophotometrically by combining the procedures of Barnes et al. (1992) and Wellburn (1994) as detailed in Palmqvist and Sundberg (2001), whereby 5–10 mg of lichen powder was extracted in $MgCO_3$-saturated dimethyl sulphoxide (DMSO) (60°C for 40 min). Equations for cyanobacterial lichens were altered because of their lack of Chl *b* (Palmqvist and Sundberg 2001).

Ergosterol analysis

Ergosterol was measured as described in detail elsewhere (Dahlman et al. 2001). For analysis, 10 mg lichen powder was mixed with 1 ml ethanol (99.5%), intensively shaken on a Vortex, and incubated on a shaker in darkness for 30 min. After centrifugation (14,000 *g*, 15 min), ergosterol was determined in the supernatant by HPLC (Waters, Milford, USA), with isocratic elution using methanol as the mobile phase. Ergosterol absorption at 280 nm was measured with a UV detector. Data were corrected for an extraction yield of 80% (Dahlman et al. 2001).

Chitin analysis

Chitin was measured in the pellet remaining after ergosterol extraction as detailed previously (Dahlman et al. 2001). The sample was treated with 0.2 M NaOH to remove proteins and amino acids that could interfere with the HPLC analysis of glucosamine. Acid hydrolysis (6 M HCl) was used to release the glucosamine residues, which were converted to fluorescent derivatives by treatment with 9-fluorenylmethylchloroformate (FMOC). The FMOC derivatives were subsequently analysed by RP-HPLC using gradient elution. Data were corrected for an extraction yield of 83% (Ekblad and Näsholm 1996).

Nitrogen analysis

Approximately 10 mg of each freeze-dried and milled lichen sample was analysed with a CHN-elemental analyser (Perkin-Elmer Model 2400 CHN). The Antarctic lichens were analysed with a Kjeltec-auto 1030 (Tectator, Stockholm, Sweden).

Statistics

Stepwise multiple linear regressions, comparison of slopes, and one-way ANOVA were made using a statistical package (Statistix 7, Analytical Software, Tallahassee, Fla, USA).

Results

Thallus nitrogen

Thallus nitrogen (N) concentrations ranged from 1 to 50 mg g^{-1} dry wt. across the lichens (Fig. 1, Appendix 1). On average, green algal lichens had the lowest, *Nostoc* lichens the highest and tripartite lichens intermediate N concentrations (Table 1). Within each photobiont group,

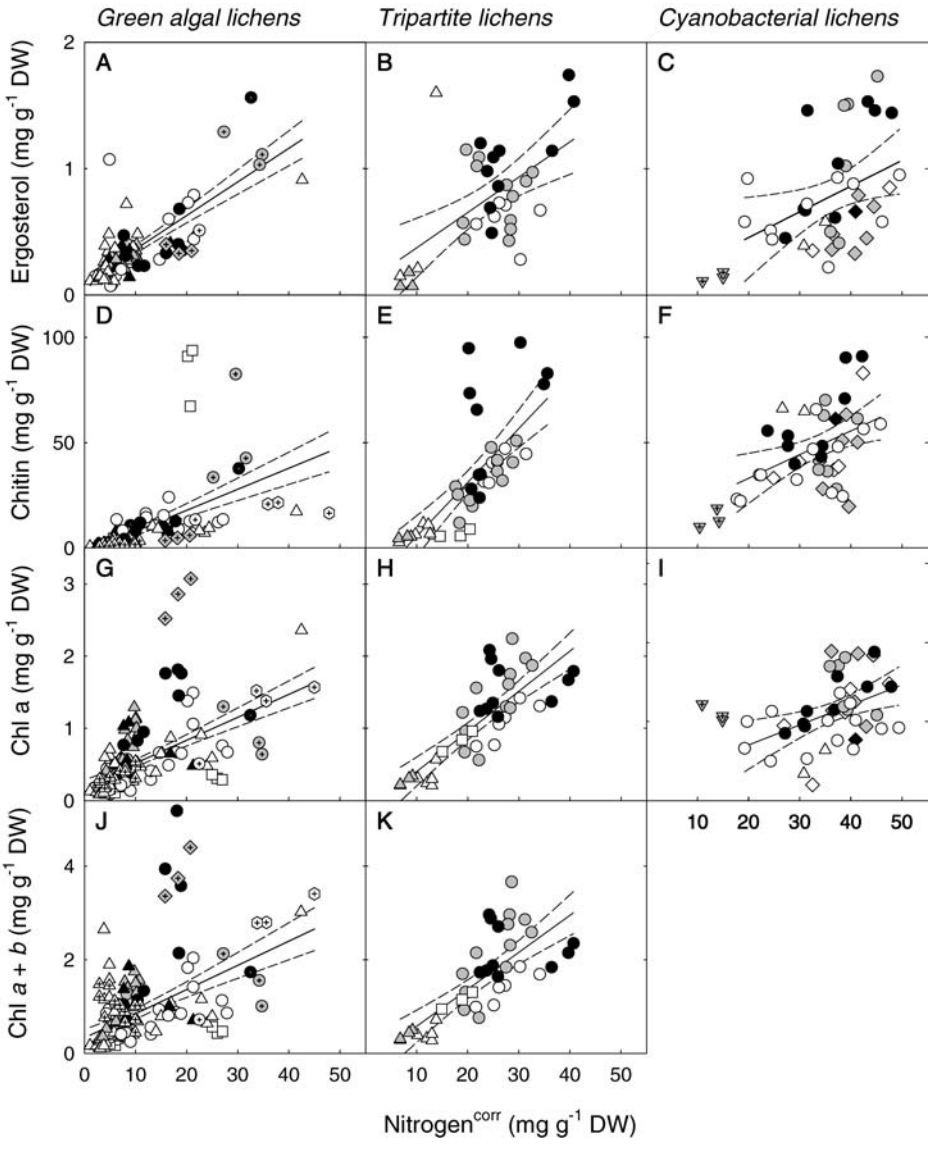

Fig. 1 The relationships between thallus nitrogen (N) and ergosterol (**A–C**), chitin (**D–F**), Chl *a* (**G–I**), or Chl *a*+*b* (**J–K**) concentrations for green algal (*A*, *D*, *G*, *J*), tripartite (*B*, *E*, *H*, *K*) and cyanobacterial (*C*, *F*, *I*) lichens. The N contents of Chl *a* (6.27% of molecular weight), or chitin (6.33% of molecular weight) were subtracted from the total thallus N (=N^{corr}) in their respective plots to avoid autocorrelation. Regression lines (±95% confidence interval) were obtained by pooling all samples in the respective plot, with the exception of N-fertilised *Hypogymnia physodes* (*grey diamond with cross*), N-fertilised *Usnea aurantiaco-atra* (*white triangle with cross*), and *Ephebe lanata* (*grey upside down triangle with cross*). Equations are given in Table 2. Colour represents habitat: *white* Arctic/Antarctic, *grey* boreal, *black* temperate/subtropical. Symbol for morphology: *square* crustose, *triangle* fruticose, *circle* foliose, *diamond* homoiomerous, with the exceptions of *Dermatocarpon* spp. (*circle with cross*), *Mastodia tesselata* (*hexagon with cross*). The Antarctic lichens are not included in the ergosterol to nitrogen plots

Table 1 Thallus nitrogen concentration (mg g^{-1} dry wt.). Lichen species included in the respective photobiont and habitat group are specified in Appendix 1. Mean values (±SD) followed by different letters are significantly different for $P<0.001$, as tested by one-way ANOVA and Tukey (HSD) comparison of means

Lichen group		Thallus nitrogen	*n*
Green algal lichens	Arctic/Antarctic	10.2±9.7 ^{A}	94
	Boreal	10.9±8.2 ^{A}	37
	Temperate/subtropical	15.7±3.7 $^{A, B}$	6
	Hypogymnia physodes (+N)	18.5±2.5 $^{A, B, C}$	3
	Usnea aurantiaco-atra (+N)	9.7±1.5 $^{A, D}$	12
Tripartite lichens	Arctic/Antarctic	19.2±8.1 $^{A, B, D}$	15
	Boreal	22.1±8.4 ^{B}	15
	Temperate/subtropical	29.0±7.1 $^{B, C}$	10
Cyanobacterial lichens	Arctic/Antarctic (*Nostoc*)	35.0±8.7 $^{C, E}$	20
	Boreal (*Nostoc*)	37.2±6.9 ^{C}	10
	Temperate/subtropical (*Nostoc*)	39.9±3.2 ^{C}	12
	Ephebe lanata (*Stigonema*)	13.7±2.3 $^{A, B, E}$	3

there was a tendency for increased N from Arctic/Antarctic to temperate/subtropical habitats. However, thallus N concentration varied extensively within each of the three photobiont groups and overlapped between the habitats, so this tendency was not statistically significant (Fig. 1, Table 1, Appendix 1).

In the green algal group, N concentrations ranged from 1 to 48 mg g^{-1} dry wt., with most below 20 mg g^{-1} dry wt. The fruticose species had the lowest and *Dermatocarpon* spp. and *Mastodia tesselata* the highest N concentrations (cf. Fig. 1G, Appendix 1). N-fertilised *Hypogymnia physodes* had ca. 20 mg N g^{-1} dry wt., which was twice the concentration of "control" thalli of this species. *Usnea aurantiaco-atra* growing in a penguin colony also had twice the N concentration found in the "control" thalli, with ca. 10 and 5 mg N g^{-1} dry wt., respectively (Appendix 1). In the tripartite group, N concentration ranged from 7 to 40 mg N g^{-1} dry wt., being lowest in the fruticose *Stereocaulon* spp. at 7–10 mg N g^{-1} dry wt. (cf. Fig. 1H, Appendix 1). In contrast to the

other lichens of this group, *Stereocaulon* has *Stigonema* and not *Nostoc* as the N_2-fixing partner (Appendix 1). The highest N concentration in this group was found in *Lobaria meridionalis*. In the cyanobacterial *Nostoc* group, N concentration ranged from 19 to 50 mg N g^{-1} dry wt. (cf. Fig. 1I), being lowest in *Nephroma expallidum* and highest in *Peltigera rufescens*. *Ephebe lanata* associated with *Stigonema* had lower a N concentration (11–15 mg g^{-1} dry wt.) than the *Nostoc* lichens (cf. Fig. 1I, Appendix 1).

Nitrogen–component relations

Concentrations of all the respective components, Chl *a* and *b*, ergosterol, and chitin, increased linearly with thallus N concentration (Fig. 1, Table 2). Ergosterol increased with 20–28 µg for each 1 mg increase in thallus N with an intercept value of 50–100 µg (Fig. 1A–C, Table 2). This relation was similar in the three photobiont groups, even though the *Nostoc* data were less well fitted to the regression equation than that of the green algal lichens. However, when the homoiomerous species was excluded, the *Nostoc* regression was improved (Table 2).

The slope of the chitin-to-N regression was similar for the green algal and the *Nostoc* lichens, while it was significantly higher for the tripartite species (Fig. 1D–F, Table 2). In the former two groups, chitin increased with 1 mg for each 1 mg increase in thallus N, while it increased with 2.6 mg for each 1 mg N in the tripartite lichens. However, the intercept of the equation was well below zero for the tripartite lichens and above zero for the *Nostoc* lichens (Table 2). Therefore, lichens in these two groups had similar chitin concentrations at the higher N concentrations, while the green algal lichens had less chitin at the highest N concentrations than the other two groups (Fig. 1D–F). As for the ergosterol-to-N relation, the *Nostoc* regression was slightly improved by excluding the homoiomerous species (Table 2). In the green algal group, *Rinodina petermanii* and one *Dermatocarpon miniatum* sample had significantly higher chitin concentrations in relation to N than the other species, while N-fertilised *H. physodes* had relatively little chitin (Fig. 1D). The chitin-to-N regression of the green algal lichens was improved from an adjusted r^2 of 0.32 to 0.61 by excluding *R. petermanii* and the odd *Dermatocarpon miniatum* sample, but the constants were not significantly altered (not shown). In the tripartite group, *Pseudocyphellaria dissimilis* had significantly more chitin in relation to N than the others (Fig. 1E). Excluding this species improved the regression from an adjusted r^2 of 0.54 to 0.82, but the constants were not significantly altered (not shown).

The Chl *a*-to-N regression had a similar slope in the green algal and the *Nostoc* lichens but was twice as high in the tripartite species (Table 2, Fig. 1G–I). It should be emphasised, however, that Chl *a* is a smaller fraction of the total content of photosynthetic chromophores in cyanobacteria than in green algae (Raven et al. 1990). The N-fertilised *H. physodes* (which was not included in any regression) had by far the highest Chl *a* concentration, being 5–6 times higher than in control samples of the same species. There were no conspicuous outliers in the tripartite group (Fig. 1H), while data were more scattered in the *Nostoc* group (Fig. 1I). *Ephebe lanata* with its *Stigonema* photobiont had Chl *a* concentrations similar to those of the *Nostoc* lichens, despite relatively low thallus N concentrations (Fig. 1I, Table 3). The Chl *a*+*b*-to-N regressions showed a pattern similar to the Chl *a*-to-N relations, with a higher slope value for tripartite lichens than for the green algal, and with the green algal group being more scattered (Table 2, Fig. 1J–K).

Despite this similar Chl *a*-to-N relation across species (Fig. 1, Table 2), the mean fraction of thallus N invested

Table 2 Regression parameters for the data presented in Fig. 1. Data [number of values] were fitted to a linear equation of the form $y=ax+b$, where y = component concentration (mg g^{-1} dry wt.), a = slope of the line (dimensionless), x = thallus nitrogen concentration (mg g^{-1} dry wt.) and b the y-axis intercept. Thallus N concentrations were corrected for the N contents of chitin and chlorophyll. All slopes were significantly different from zero for $P<0.001$ if not otherwise stated after the adjusted r^2 value. Slope values followed by a different letter or number are significantly different for each component-to-N regression for $P<0.001$, if not stated otherwise after the slope value. Each respective compound-to-N correlation was tested between the photobiont groups, but not to each other

Correlation	Regression	Green	Tripartite	Nostoc all	Nostoc heteromerous
Ergosterol–nitrogen	a	0.026[A]	0.028 [A]	0.020 [A]	0.027 [A]
	b	0.1	0.1	0.05	–0.1
	Adjusted r^2	0.61 [92]	0.31 [34]	0.11; P=0.02 [36]	0.23; P=0.007 [27]
Chitin–N^{corr}	a	1.0 [a]	2.6 [b]	1.1 [a]	1.2 [a]
	b	–2.2	–20±8.3	10±13	10±15
	Adjusted r^2	0.32 [134]	0.54 [40]	0.15; P=0.006 [41]	0.18; P=0.01 [29]
Chla–N^{corr}	a	0.031 [1]	0.056 [2]	0.025 [1]	
	b	0.2	–0.2	0.2	
	Adjusted r^2	0.43 [137]	0.64 [40]	0.16; P=0.004 [42]	
Chl a+b–N^{cor}	a	0.05 [x]	0.08 [y] P=0.038	Without Chl b	
	b	0.3	–0.2		
	Adjusted r^2	0.31 [137]	0.55 [40]		

Table 3 Fraction of thallus nitrogen (N) (percent total thallus N) invested in chlorophyll *a* pigment as a function of photobiont and morphology, where the N content of Chl *a* was calculated using the molar fraction of N in this pigment (6.27%). Lichen species included in each group are specified in Appendix 1. Mean values (±SD) followed by different letter or numbers are significantly different for $P<0.05$ as tested by one-way ANOVA and Tukey (HSD) comparison of means. The Arctic material was tested separately from the Antarctic because no gas exchange data were available for the former. Antarctic lichens and the rest were also tested separately. The outlier species (see Materials and methods) were not included in the analysis (*Bor/temp/sub* Boreal/temperate/subtropical)

Lichen group			Chl *a* (N)	*n*
Arctic lichens	Green algal lichens	Crustose	0.14±0.00^{A,B,C}	2
		Fruticose	0.34±0.11^{A,B}	32
		Foliose	0.38±0.15^{A}	15
	Tripartite lichens	Fruticose	0.21±0.04^{A,B,C}	3
		Foliose	0.24±0.03^{A,B,C}	6
	Nostoc lichens	Fruticose	0.10±0.04^{B}	2
		Foliose	0.16±0.08^{C}	12
Antarctic lichens	Green algal lichens	Crustose	0.13±0.07^{a}	6
		Fruticose	0.36±0.23^{b}	24
		Foliose	0.21±0.06^{a,b}	15
	Tripartite lichens	Crustose	0.28±0.006^{a,b}	3
		Fruticose	0.12±0.03^{a,b}	3
	Nostoc lichens	Foliose	0.20±0.03^{a,b}	6
	Outlier species	Usnea aurantiaco-atra (+N)	0.35±0.13	12
Bor/temp/sub	Green algal lichens	Fruticose	0.49±0.18^{1}	24
		Foliose	0.46±0.18^{1,2}	19
	Tripartite lichens	Fruticose	0.22±0.02^{3,4}	3
		Foliose	0.35±0.10^{2,3}	22
	Nostoc lichens	Foliose	0.22±0.06^{4}	22
	Outlier species	Hypogymnia physodes (+N)	0.96±0.04	3
		Ephebe lanata (*Stigonema*)	0.53±0.15	3

in Chl *a* varied at least fivefold when the lichens were grouped according to photobiont and morphology (Table 3). Relative nitrogen investments in Chl *a* were generally highest in foliose and fruticose green algal lichens (0.21–0.49%) and lowest in foliose *Nostoc* lichens (0.16–0.22%), with tripartite lichens in between. This trend was found among the Arctic and the boreal/temperate/subtropical samples but not among the Antarctic lichens (Table 3). Consistent with the above findings that N-fertilised *H. physodes* had low ergosterol and low chitin concentrations but high Chl *a*, these had invested as much as 0.96% of their thallus N in Chl *a* pigments (Table 3).

CO_2 gas exchange

Light-saturated net photosynthesis (NP_{max}) varied between 0.1 and 15 nmol CO_2 s^{-1} g^{-1} dry wt., and steady state respiration (R) between 0.1 and 2.4 nmol CO_2 s^{-1} g^{-1} dry wt. among the Antarctic lichens, when measurements were made at 5°C (Fig. 2). For these, NP_{max} could be predicted by a simple linear equation of the form NP = 3.8[R] + 0.07 (Table 4), while R was best predicted by R = 0.10[NP_{max}] + 0.02[N] + 0.31 (Table 5). This implies that both R and NP_{max} were more strongly related to each other than to the other measured components. However, the model indicates that R was also dependent on N status, and both NP_{max} and R increased significantly with Chl *a* concentration (Fig. 2). The highest NP_{max} and R rates were then generally achieved by thalli with the highest N and Chl *a* statuses. An exception to this was the tripartite lichen *Placopsis contortuplicata* and green algal *Xanthoria candelaria*, which had higher rates of NP_{max} in relation to their Chl *a* concentration than the others (Fig. 2). However, the unexpectedly high NP rates

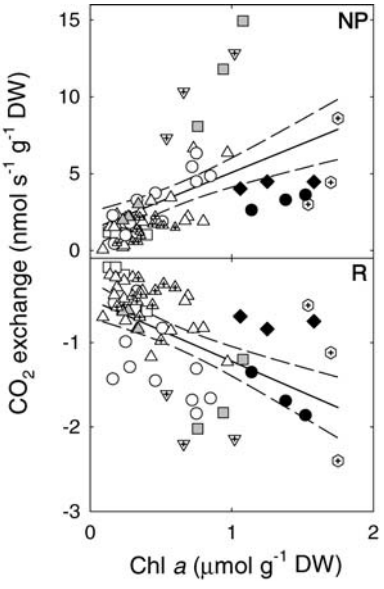

Fig. 2 Light-saturated net CO_2 fixation (*NP*) and dark CO_2 efflux (*R*) rates as a function of thallus Chl *a* concentration of the Antarctic lichens measured at ambient CO_2 and 5°C. All samples with the exception of N-fertilised *Usnea aurantiaco-atra* (*triangle with cross*) were pooled in a regression analysis (straight line) yielding the following linear equations; NP = 3.8±0.8[Chl *a*] + 1.3±0.6 with adj r^2=0.27 and P=0.0000, and R = 0.73±0.15[Chl *a*] + 0.49±0.11 with adj r^2=0.30 and P=0.0000. Regression line given with ±95% confidence interval. Colours represent photobiont group: *white* green bipartite, *grey* tripartite, *black Nostoc* bipartite. Symbol for morphology: *square* crustose, *triangle* fruticose, foliose, *diamond* -homoiomerous, with the exceptions of *Placopsis contortuplicata* (*grey squares*), *Xanthoria candelaria* (*upside down triangle with cross*), *Mastodia tesselata* (*hexagon with cross*)

Table 4 Stepwise multiple linear regression of photosynthetic net CO_2 fixation (nmol s^{-1} g^{-1} dry wt., dependent variable) using thallus nitrogen concentration (mg g^{-1} dry wt.), Chl *a* concentration (μmol g^{-1} dry wt.), steady state respiration (nmol s^{-1} g^{-1} dry wt.), and the fraction of thallus N invested in Chl *a* (Chl *a* [N]; percent of total N) as independent variables. The three photobiont groups were pooled in the respective analysis, with the exception of *Ephebe lanata* that has *Stigonema* (Appendix 1), N-fertilised *Hypogymnia physodes*, and "penguin colony" *Usnea aurantiaco-atra*. In all cases, backward and forward elimination of variables resulted in identical models (*Bor/temp/sub* Boreal/temperate/subtropical)

Lichen group	Resulting best subset model							
	Variable	Coefficient±SE	Student's *t*	*P* Variable	F	adj r^2	*P* Regression	*n*
Antarctic (5°C)	Constant	0.07±0.56	0.12	0.9045				
	R5	3.8±0.51	7.36	0.0000	54	0.49	0.0000	57
Borl/temp/sub (10°C)	Constant	–2.6±2.8	–0.93	0.3540				
	Chl *a* [N]	16.0±5.3	3.01	0.0036				
	Chl *a*	8.3±1.5	5.42	0.0000	20	0.33	0.0000	80
Bor/temp/sub (15°C)	Constant	–16.1±5.4	–2.98	0.0038				
	Nitrogen	0.43±0.13	3.25	0.0017				
	R15	0.98±0.39	2.49	0.0147				
	Chl *a* [N]	47.0±8.9	5.28	0.0000	15	0.32	0.0000	90

Table 5 Stepwise multiple linear regression of steady-state respiration (nmol s^{-1} g^{-1} dry wt., dependent variable) using thallus nitrogen concentration (mg g^{-1} dry wt.), Chl *a* concentration (μmol g^{-1} dry wt.), ergosterol concentration (μmol g^{-1} dry wt.), photosynthetic net CO_2 fixation (nmol s^{-1} g^{-1} dry wt.), and the fraction of thallus N invested in Chl *a* (Chl *a* [N]; percent of total N), as independent variables. Ergosterol was not included in the Antarctic lichen regression. The three photobiont groups were pooled in the respective analysis, with the exception of *Ephebe lanata* which has *Stigonema* (Appendix 1), N-fertilised *Hypogymnia physodes* and "penguin colony" *Usnea aurantiaco-atra*. In all cases, backward and forward elimination of variables resulted in identical models (*Bor/temp/sub* Boreal/temperate/subtropical)

Lichen group	Resulting best subset model							
	Variable	Coefficient±SE	Student's *t*	*P* Variable	F	adj r^2	*P* Regression	*n*
Antarctic (5°C)	Constant	0.31±0.09	3.45	0.0011				
	Nitrogen	0.02±0.005	3.42	0.0012				
	NP5	0.10±0.02	5.67	0.0000	40	0.57	0.0000	57
Bor/temp/sub (10°C)	Constant	2.7±0.78	3.48	0.0008				
	Chl *a*	2.81±0.42	6.67	0.0000				
	Chl *a* [N]	–3.8±1.5	–2.63	0.0103	25	0.37	0.0000	80
Bor/temp/sub (15°C)	Constant	4.72±0.91	5.15	0.0000				
	Chl *a*	2.76±0.56	4.91	0.0000				
	NP15	0.06±0.03	2.49	0.0146				
	Chl *a* [N]	–6.0±1.8	–3.36	0.0012	19	0.38	0.0000	90

of the crustose *P. contortuplicata* may be an overestimation because the thallus was removed from its substrate after the measurements, and some material may be missing in the dry weight determinations.

For the rest of the lichens, i.e. the boreal/temperate/subtropical lichens, and when measurements were made at 10°C, NP was best predicted by an equation including both the absolute concentration of Chl *a* and the fraction of thallus N invested in Chl *a* (Chl *a*[N]), where NP increased when these two parameters increased (Table 4). Respiration was also best predicted by the same two parameters. However, in this equation, R decreased with increasing Chl *a*[N] but increased with the absolute concentration of Chl *a* (Table 5). At 15°C, R varied between 1 and 16 and NP between –2 and 81 nmol CO_2 s^{-1} g^{-1} dry wt. for the rest of the lichens (Fig. 3). At this temperature, NP_{max} was best predicted by an equation including R, thallus N and Chl *a*[N], when all samples except for *Ephebe lanata* and the N-fertilised *H. physodes* were included (Table 4). Again, NP increased when the included parameters increased. Respiration at 15°C was also best predicted by a multiple linear equation including Chl *a*, NP and Chl *a*[N] (Table 5), where R and Chl *a*[N] were again negatively related. One *Peltigera horizontalis* thallus displayed a slightly negative NP rate at both 10 and 15°C caused by a relatively high rate of respiration. *D. miniatum* and *E. lanata* also displayed relatively low NP rates in relation to their R (Fig. 3), while one *Sphaerophorus globosus* sample had a very low R in relation to its NP. The reasons for these deviations were not obvious and as the various regressions were little altered by excluding these samples (not shown), the samples were retained.

Table 6 Average photosynthetic efficiency quotient [K_F=(NP_{max}+R)/R] as a function of photobiont and morphology. Lichen species included in each group are specified in Appendix 1. Mean values (±SD) followed by different letters are significantly different for P<0.05 as tested by one-way ANOVA and Tukey (HSD) comparison of means. The Antarctic material was tested separately from the rest of the lichens. The outlier species (see Materials and methods) were not included in the analysis (*Bor/temp/sub* Boreal/temperate/subtropical)

Lichen group			K_F	n
Antarctic lichens	Green algal lichens	Crustose	7.5±4.4[A]	6
		Fruticose	5.4±2.3[A]	24
		Foliose	4.1±1.9[A]	15
	Tripartite lichens	Crustose	8.6±4.4[A]	3
		Fruticose	4.4±0.3[A]	3
	Nostoc lichens	Foliose	4.8±2.1[A]	6
	Outlier species	Usnea aurantiaco-atra (+N)	3.9±1.5	12
Bor/temp/sub	Green algal lichens	Fruticose	5.7±3.61	24
		Foliose	4.0±2.11[2]	19
	Tripartite lichens	Fruticose	2.4±0.41[2]	3
		Foliose	3.3±1.52	22
	Nostoc lichens	Foliose	3.3±1.62	22
	Outlier species	Hypogymnia physodes (+N)	5.1±0.5	3
		Ephebe lanata (*Stigonema*)	1.1±0.3	3

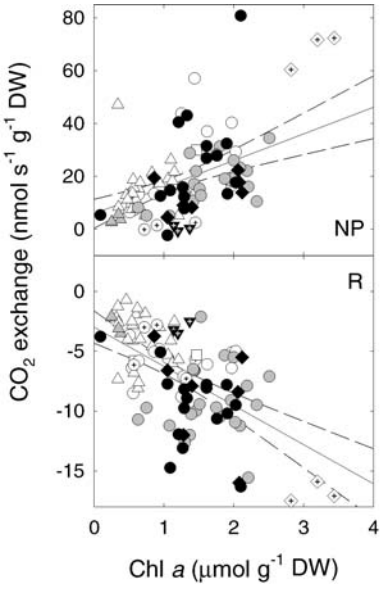

Fig. 3 Light-saturated net CO_2 fixation (*NP*) and dark CO_2 efflux (*R*) rates as a function of thallus Chl *a* concentration of the boreal and temperate/subtropical lichens measured at ambient CO_2 and 15°C. All samples with the exception of N-fertilised *Hypogymnia physodes* (*white diamond with cross*) and *Ephebe lanata* (*black upside-down triangle with cross*) were pooled in the regression analysis (straight line) yielding the following linear equations; NP = 10.1±2.1[Chl *a*] + 5.9±2.8 with adj r^2=0.20 and P=0.0000, R = 3.3±0.5[Chl *a*] + 3.0±0.7 with adj r^2=0.30 and P=0.0000. Regression line given with ±95% confidence interval. Colour represents photobiont group: green bipartite, *grey* tripartite, *black Nostoc* bipartite. Symbols for morphology: *square* crustose, *triangle* fruticose, *circle* foliose, *diamond* homoiomerous, with the exception of *Dermatocarpon* spp. (*circle with cross*)

On average, the photosynthetic efficiency quotient [K_F = (NP_{max}+R/R)] was similar in the Antarctic lichens and the rest of the lichens, even though the former were measured at 5°C and the latter at 15°C (Table 6). However, there was a tendency for higher K_F values in the Antarctic lichens, which might be expected because R increases more than P with increasing temperature (Kappen 1988). For the Antarctic lichens, there was no significant difference in K_F between the photobiont/morphology groups ranging from 4.1 to 8.6 (Table 6). This agrees with the NP and R equations for the Antarctic lichens (Tables 4, 5), yielding theoretical K_F values of 4.8–5.5 for their range of NP and R rates (Fig. 2). For the rest of the lichens, K_F was highest in the fruticose, green algal lichens (5.7), and lowest in the foliose *Nostoc* lichens (3.3) (Table 6). This might also be expected because relative N investments in Chl *a* were also highest in the fruticose green algal lichens and lowest in the foliose *Nostoc* lichens (Table 3). This and the fact that NP increased and R decreased with increasing Chl *a*[N] (Tables 4, 5) predicts a higher K_F for the former than for the latter group of lichens.

Discussion

Photobiont to mycobiont ratios

The positive correlation between each of the three components and thallus N (Fig. 1, Table 1) supports previous investigations both inter- (Green et al. 1997; Palmqvist et al. 1998; Sundberg et al. 1999) and intraspecific (Sundberg et al. 2001). The Chl *a*-to-ergosterol ratio remained surprisingly similar across the lichens with an average of 1.8±1.1 (w:w), so the ratio of photobiont cells to metabolically active fungal biomass was relatively similar across the lichens irrespective of N status. However, the homoiomerous *Nostoc* species had more Chl *a* and less ergosterol than might be predicted from their N statuses (Fig. 1), indicating a higher photobiont to mycobiont ratio in these, as also supported in the literature (Hawksworth and Hill 1984). The N-fertilised *Hypogymnia physodes* thalli also had an increased photobiont to mycobiont ratio because both the Chl *a*-to-ergosterol and the Chl *a*-to-chitin ratio were high (Fig. 1) and a much larger proportion of their thallus N resources were invested in Chl *a* than in control thalli (Table 3). The lower ergosterol concentration of thalli with relatively little mycobiont biomass supports the concept that ergosterol is a representative marker for the fungal plasma membrane alone (Ekblad and Näsholm 1996); see also

the discussion in Sundberg et al. (1999). Despite the balanced Chl *a*-to-ergosterol ratio, chitin concentrations relative to thallus N were higher in both bi- and tripartite lichens with *Nostoc* than in the majority of the bi-partite green algal lichens (Fig. 1, Table 2). This might reflect a different composition of the cell wall in *Nostoc*-containing compared to green algal lichens, with higher chitin concentrations in relation to other cell wall components in *Nostoc* associations, as shown by Boissière (1987).

Carbon gain capacity

We obtained NP_{max} values for the lichens at the time of their collection and compared these rates for all samples measured at the same temperature. When related to thallus dry weight, NP_{max} varied 60-fold among the Antarctic samples at 5°C (Fig. 2) and 50-fold among the rest of the lichens at 15°C (Fig. 3). A significant fraction of this variation could be explained by the variation in Chl *a* across samples (Figs. 2, 3), supported by previous investigations showing a correlation between total chlorophyll and photosynthetic capacity of lichens (Tretiach and Carpanelli 1992; Tretiach and Pecchiari 1995; Valladares et al. 1996; Green et al. 1997). However, the present study emphasises that Chl *a* alone predicts NP_{max} better than total chlorophyll, which agrees with a broad range of other phototrophs (Enriquez et al. 1996). However, the use of Chl *a* as a marker for photosynthetic capacity across lichens is somewhat constrained due to the inherent differences in chromophore composition of cyanobacteria versus green algae (Raven et al. 1990). Moreover, Chl *a* concentration did not explain all of the variation in NP_{max} across the lichens, and a more significant part could be accounted for when the fraction of total thallus N invested in Chl *a* (Chl *a*[N]) was also included as a factor (Table 4). The positive relation between NP_{max} and Chl *a* and/or Chl *a*[N] does not necessarily imply that lichen photosynthesis is primarily limited by pigment concentration per se (see Raven 1992). This rather emphasises that overall investments in photosynthetic capacity co-varies with Chl *a*. The N costs of Chl *a* pigments are in fact very low in comparison to the N requirements of other photosynthetic components, where the proteins of the two photosystems and their light-harvesting antennae require 25–30 times more N and the Calvin cycle proteins 15–20 times more N than their associated Chl *a* (Chapin et al. 1987). Of these proteins, the primary carboxylating enzyme Rubisco is dominating with respect to abundance and N costs, followed by the light-harvesting proteins. Some of the unaccounted for variation in NP_{max} might then be related to variation in amount and activity of Rubisco (cf. Palmqvist 2000; MacKenzie et al. 2001). Finally, temperature has a large impact on lichen photosynthesis (Kershaw 1985; Kappen 1988) and it is likely that the unaccounted for variation in NP_{max} across the lichens would have been lower if all samples had been measured at their optimal temperature.

Carbon expenditures and regulation of carbon balance

Respiration functions to energise growth, transport, and assimilation processes and convert assimilated carbon into substances that can be used for growth and maintenance (Lambers et al. 1998). Because respiration is so complex, CO_2 efflux characteristics of whole individuals can not tell us how all these subprocesses are regulated, or which process is dominating (cf. Palmqvist 2000). However, as for the carbon gain capacity, we wanted comparable values of carbon expenditures for these lichens. This was achieved by allowing the lichens to reach a steady-state rate of CO_2 release after any transient bursts resulting from sudden rehydration or temperature changes (cf. Kershaw 1985; Sundberg et al. 1999). When related to thallus dry weight, this R varied 10- to 15-fold across species, both among the Antarctic lichens at 5°C (Fig. 2) and for the rest of the lichens at 15°C (Fig. 3). A similar variation has been recorded for plant leaves representing various biomes, functional groups, and leaf N statuses similar to those of the lichens investigated here (Reich et al. 1998). For the Antarctic species, the variation in R was best explained by the variation in NP_{max} together with thallus N concentration, accounting for 57% of the variation (Table 5). In these, Chl *a* alone accounted for 30% of the variation in R (Fig. 2). For the rest of the lichens, R was positively related to Chl *a* and positively related to NP_{max}, while being negatively effected by Chl *a*[N]. These variables together explained 38% of the variation in R at 15°C (Table 5).

However, respiration also varies significantly with temperature, with the potential to acclimate to prevailing temperatures in the particular habitat (Kershaw 1985; Lambers et al. 1998). Moreover, respiration increases linearly, while photosynthesis generally shows an optimal response in relation to increasing temperature (Kershaw 1985; Kappen 1988). Once again, this emphasises that it would have been better to measure the gas-exchange properties of all the lichen samples at their respective optimal temperatures, as for the Antarctic lichens. Nevertheless, despite this constraint in the data set, 13% of the variation in R could be explained by the variation in NP_{max} alone for the rest of the lichens at 15°C (not shown). The positive correlation between NP_{max} and R around a similar equilibrium across lichens provides evidence for a regulatory control of these two processes in relation to each other. The relatively low variation in K_F across species gives further support for this (Table 6), even though the nature of this regulation cannot be deduced from our data. Further analyses of already published in situ and long-term CO_2 gas-exchange characteristics of various lichens (cf. Lange et al. 1994; Zotz et al. 1998) might provide additional evidence for covariation of NP and R in lichens. In plants, it has long been established that the magnitude of photosynthetic and respiratory activity covaries with each other (Enriquez et al 1996; Lambers et al. 1998). The general view is that photosynthesis is feed-back inhibited by carbohydrate demands rather than vice versa (cf. Lambers

et al. 1998). Assuming that the mycobiont is the largest carbon sink in lichens, we may then speculate that the fungus is somehow able to control carbohydrate availability by regulating the size of its photobiont population. The idea that the mycobiont exerts regulatory control over the photobiont goes back to Schwendener, who in 1867 proposed the dual nature of lichens (see Richardson 1999), and much evidence tends to support this viewpoint (cf. Honegger 1991; Hill 1992; Hyvärinen et al. 2002).

The data presented here also show that R increases with thallus nitrogen status either directly, as for the Antarctic lichens (Table 5), or indirectly because of the correlation between nitrogen and Chl *a* (Fig. 1, Table 5). This emphasises that lichen mycobionts that require high levels of nitrogen, such as members of the Peltigerales, must form a thallus providing space for a large enough photobiont population to meet its concomitantly high carbohydrate demands (Hyvärinen et al. 2002). Moreover, a mycobiont with high carbohydrate requirements must also ensure sufficient nitrogen investments in the photobiont population to achieve efficient photosynthesis. However, there are few investigations on resource flow within lichen thalli, and nutrient flow from myco- to photobiont remains to be demonstrated (cf. Richardson 1999). In this context, the negative correlation between R and Chl *a*[N] found for the rest of the lichens at 15°C (Table 5) is interesting and merits further studies on the regulation of resource flow in different lichen associations. This finding implies that respiration rate per unit nitrogen is lower if this N is present in photosynthetic components than other N compounds in the thallus. This further suggests that a lichen that can increase the number of photobionts with increasing N supply should be able to grow faster, supported by a higher efficiency of light energy conversion to lichen biomass with increasing Chl *a* concentration in the thallus (Palmqvist and Sundberg 2000; Sundberg et al. 2001). However, N fertilisation of lichens can also reduce their vitality and may cause reduced rates of area expansion (Sundberg et al. 2001; Dahlman et al. 2002). It must, therefore, be emphasised that the relationships established here reflect broad-scale patterns across lichens and discussions concerning likely responses of a particular lichen to varying N supply will require more detailed intraspecific studies. Nevertheless, it appears that a functional carbon to nitrogen equilibrium model (Brouwer 1962) is also applicable to lichens, with N being invested so that maximal C input capacity matches respiratory C demand around a similar (positive) equilibrium across species.

Acknowledgements FORMAS, Sweden provided grants (24.0795/97) to K.P. Center for Environmental Research (CMF, Umeå, Sweden No 993194) and the J.C. Kempe Foundation provided grants to L.D. Vetenskapsrådet (The Swedish Research Council) provided a grant to A.T. (B-BU9702–302). The Spanish CICYT gave financial support for the 1997 Antarctic expedition of F.V. (ANT 99–0680-C02–01). The Swedish Polar Research Secretariat gave us the opportunity to participate in the TNW99 expedition. Martin Westberg, Lund University, collected lichens during the second leg of TNW99. Karl-Erik Renhorn, Umeå University, Sweden, collected and identified the lichens from boreal Sweden and Tenerife. Bodil Sundberg, Örebro University, Sweden, collected lichens in South Africa and took part in the initiation of this study. Göran Thor, Uppsala, Sweden, collected Japanese material and gave taxonomic advice during initial discussions. Torgny Näsholm, Margareta Zetherström and Jörgen Persson, SLU, Umeå, Sweden, helped with HPLC analysis and improved ergosterol and chitin extraction protocols. Sune Linder, SLU Uppsala, Sweden is acknowledged for allowing us to collect lichens from the Flakaliden experimental site.

Appendix 1

Species names of the investigated lichens, photobiont affiliation, morphology, origin and thallus nitrogen concentration range (mg g^{-1} dry wt.). (*G* green alga, *Nos* Nostoc, *Stig* Stigonema, *Tri* tripartite, *Cru* crustose, *CruHom* homoiomerous and crustose, *Fol* foliose, *Fru* fruticose, *Ant* Antarctica, *Arc* Arctic Canada, *Bor* Boreal, *Temp* temperate, *nm* not measured)

Lichen association	Photobiont, morphology, origin	Thallus N range
Bryoria furcellata	G, Fru, Bor	8–11
Caloplaca elegans	G, Fol, Ant	19–28
Cetraria islandica	G, Fru, Arc	3–4
Cetrariella delisei	G, Fru, Arc	3–6
Cladonia pyxidata	G, Fru, Ant	6–8
Collema sp.	Nos, CruHom, Bor, Temp	36–42
Dactylina arctica	G, Fru, Arc	3
Dactylina beringica	G, Fru, Arc	5–6
Dactylina ramulosa	G, Fru, Arc	3–5
Degelia atlantica	Nos, Fol, Temp	nm
Dermatocarpon miniatum	G, Fol, Bor, Temp	27–35
Dermatocarpon sp.	G, Fol, Arc	22
Diploshistes scruposus	G, Cru, Bor	nm
Ephebe lanata	Stig, Fru, Bor	11–15
Evernia prunastri	G, Fru, Bor	10
Flavocetraria cucullata	G, Fru, Arc	2–7
Flavocetraria nivalis	G, Fru, Arc	3–5
Himantormia lugubris	G, Fru, Ant	4–5
Hypogymnia physodes	G, Fol, Bor	6–8
Hypogymnia physodes N	G, Fol, Bor and N-fertilised	16–21
Lasallia sp.	G, Fol, Temp	16–19
Leptogium puberulum	Nos, CruHom, Ant	27–40
Leptogium saturninum	Nos, CruHom, Arc, Bor	33–48
Lobaria meridionalis	Tri, Fol, Temp	37–41
Lobaria pulmonaria	Tri, Fol, Bor, Temp	19–29
Mastodia tesselata	G, Fol, Ant	36–48
Nephroma arcticum	Tri, Fol, Bor	19–22
Nephroma bellum	Nos, Fol, Bor	36–39
Nephroma expallidum	Nos, Fol, Arc	19–20
Nephroma sp.	Nos, Fol, Temp	32–38
Ochrolechia antarctica	G, Cru, Ant	5–6
Pannaria rubiginosa	Nos, Fol, Temp	37
Parmelia saxatilis	G, Fol, Ant, Arc	5–9(Ant); 20–21(Arc)
Parmotrema arnoldii	G, Fol, Temp	8
Parmotrema sp.	G, Fol, Temp	10–19
Peltigera aphthosa	Tri, Fol, Arc, Bor	22–33
Peltigera canina	Nos, Fol, Arc, Bor	36–46
Peltigera didactyla	Nos, Fol, Ant	38–41
Peltigera horizontalis	Nos, Fol, Temp	27–31
Peltigera leucophlebia	Tri, Fol, Arc	26–34

Lichen association	Photobiont, morphology, origin	Thallus N range
Peltigera membranacea	Nos, Fol, Arc	24–31
Peltigera rufescens	Nos, Fol, Arc	25–50
Physcia caesia	G, Fol, Ant, Arc	13–18
Placopsis contortuplicata	Tri, Cru, Ant	15–21
Pseudephebe pubescens	G, Fru, Ant	5–7
Pseudocyphellaria aurata	Tri, Fol, Temp	25–26
Ramalina cuspidata	G, Fru, Temp	7–9
Ramalina fastigiata	G, Fru, Temp	6
Ramalina fraxinea	G, Fru, Temp	7–8
Ramalina terebrata	G, Fru, Temp	14–17
Rhizocarpon geographicum	G, Cru, Bor	nm
Rinodina petermanii	G, Cru, Ant	25–27
Roccella fuciformis	G, Fru, Temp	17–21
Roccella sp.	G, Fru, Temp	8
Solorina crocea	Tri, Fol, Bor	28
Sphaerophorus globosus	G, Fru, Ant, Arc, Bor	1–4
Stereocaulon alpinum C	Tri, Fru, Ant	12–13
Stereocaulon sp.	Tri, Fru, Arc, Bor	7–14
Sticta artica	Nos, Fol, Arc	31–35
Sticta canariensis	Nos, Fol, Temp	43–48
Teloschistes flavicans	G, Fru, Temp	5–9
Thamnolia vermicularis	G, Fru, Arc, Bor	4–8
Umbilicaria Ant	G, Fol, Ant	7–9
Umbilicaria cylindrica?	G, Fol, Arc	15
Umbilicaria leiocarpa	G, Fol, Arc	5–6
Umbilicaria lyngeii	G, Fol, Arc	5
Umbilicaria proboscidea	G, Fol, Arc	4–5
Umbilicaria sp.	G, Fol, Arc	6
Umbilicaria virgins	G, Fol, Arc	9
Usnea antarctica	G, Fru, Ant	5–6
Usnea aurantiaco-atra	G, Fru, Ant	4–5
Usnea aurantiaco-atra N	G, Fru, Ant and N-fertilised	8–11
Usnea hirta	G, Fru, Bor	8–10
Vulpicida tilesii	G, Fru, Arc	3–4
Xanthoria candelaria	G, Fru, Ant	23–25
Xanthoria elegans	G, Fol, Arc	7–21

References

Barnes JD, Balaguer L, Manrique E, Elvira S, Davison AW (1992) A reappraisal of the use of DMSO for the extraction and determination of chlorophyll *a* and *b* in lichens and higher plants. Environ Exp Bot 32:85–100

Boissière J-C (1987) Ultrastructural relationship between the composition and the structure of the cell wall of the mycobiont of two lichens. Bibl Lichenol 25:117–132

Brouwer R (1962) Distribution of dry matter in the plant. Neth J Agric Sci 10:399–408

Campbell D, Hurry V, Clarke AK, Gustafsson P, Oquist G (1998) Chlorophyll fluorescence analysis of cyanobacterial photosynthesis and acclimation. Microbiol Mol Biol Rev 62:677–683

Chapin III FS (1991) Integrated responses of plants to stress. BioScience 41: 29–36

Chapin III FS, Bloom AJ, Field CB, Waring RH (1987) Plant responses to multiple environmental factors. BioScience 37:49–57

Dahlman L, Zetherström M, Sundberg B, Näsholm T, Palmqvist K (2001) Measuring ergosterol and chitin in lichens. In: Kranner I, Beckett R, Varma A (eds) Protocols in lichenology-culturing, biochemistry, physiology and use in biomonitoring. Springer, Berlin Heidelberg New York, pp 348–362

Dahlman L, Näsholm T, Palmqvist K (2002) Growth, nitrogen uptake, and resource allocation in the two tripartite lichens *Nephroma arcticum* and *Peltigera aphthosa* during nitrogen stress. New Phytol 153:307–315

Ekblad A, Näsholm T (1996) Determination of chitin in fungi and mycorrhizal roots by an improved HPLC analysis of glucosamine. Plant Soil 178:29–35

Elix JA (1996) Biochemistry and secondary metabolites. In: Nash TH III (ed) Lichen biology. Cambridge University Press, Cambridge, pp 154–180

Enriquez S, Duarte CM, Sand-Jensen K, Nielsen SL (1996) Broad-scale comparison of photosynthetic rates across phototrophic organisms. Oecologia 108:197–206

Eriksson O, Winka K (1998) Families and higher taxa of Ascomycota. Myconet 1:17–24

Feige GB, Jensen M (1992) Basic carbon and nitrogen metabolism of lichens. In: Reisser W (ed) Algae and symbioses: plants, animals, fungi, viruses, interactions explored. Biopress, Bristol, pp 277–299

Gargas A, DePriest PT, Grube M, Tehler A (1995) Multiple origin of lichen symbiosis in fungi suggested by SSU rDNA phylogeny. Science 268:1492–1495

Grace J (1997) Toward models of resource allocation by plants. In: Bazzaz FA, Grace J (eds) Plant resource allocation. Academic, San Diego, pp 279–291

Green TGA, Büdel B, Meyer A, Zellner H, Lange OL (1997) Temperate rainforest lichens in New Zealand: light response of photosynthesis. NZ J Bot 35:493–504

Hawksworth DL, Hill DJ (1984) The lichen forming fungi. Blackie, Glasgow

Hill DJ (1992) The co-ordination of development of symbionts in mutualistic symbiosis with reference to the cell cycle of the photobiont in lichens. Symbiosis 14:325–333

Honegger R (1991) Functional aspects of the lichen symbiosis. Annu Rev Plant Physiol Plant Mol Biol 42:553–578

Honegger R (1996a) Mycobionts. In: Nash TH III (ed) Lichen biology. Cambridge University Press, Cambridge, pp 24–36

Honegger (1996b) Morphogenesis. In: Nash TH III (ed) Lichen biology. Cambridge University Press, Cambridge, pp 65–87

Hyvärinen M, Härdling R, Tuomi J (2002) Cyanobacterial lichen symbiosis: the fungal partner as an optimal harvester. Oikos (in press)

Kappen L (1988) Ecophysiological relationships in different climatic regions. In: Galun M (ed) Handbook of lichenology 2. CRC, Boca Raton, Fla, pp 37–100

Kershaw KA (1985) Physiological ecology of lichens. Cambridge University Press, Cambridge

Lambers H, Chapin III FS, Pons TL (1998) Plant physiological ecology. Springer, Berlin Heidelberg New York

Lange OL, Büdel B, Zellner H, Zotz G, Meyer A (1994) Field measurements of water relations and CO_2 exchange of the tropical, cyanobacterial basidiolichen *Dictyonema glabratum* in a Panamian Rainforest. Bot Acta 107:279–290

Lange OL, Green TGA, Heber U (2001) Hydration-dependent photosynthetic production of lichens: what do laboratory studies tell us about field performance? J Exp Bot 52:2033–2042

Mackenzie TDB, MacDonald TM, Dubois LA, Campbell DA (2001) Seasonal changes in temperature and light drive acclimation of photosynthetic physiology and macromolecular content in *Lobaria pulmonaria* Planta 214:57–66

Nash TH III (1996) Nutrients, elemental accumulation and mineral cycling. In: Nash TH III (ed) Lichen biology. Cambridge University Press, Cambridge, pp 136–153

Palmqvist K (1993) Photosynthetic CO_2 use efficiency in lichens and their isolated photobionts: the possible role of a CO_2 concentrating mechanism in cyanobacterial lichens. Planta 191:48–56

Palmqvist K (2000) Carbon economy in lichens. New Phytol 148:11–36

Palmqvist K, Sundberg B (2000) Light use efficiency of dry matter gain in five macro-lichens: relative impact of microclimate conditions and species-specific traits. Plant Cell Environ 23:1–14

Palmqvist K, Sundberg B (2001) Characterizing photosynthesis and respiration in freshly isolated or cultured lichen photobionts. In: Kranner I, Beckett R, Varma A (eds) Protocols in lichenology-culturing, biochemistry, physiology and use in biomonitoring. Springer, Berlin Heidelberg New York, pp 152–181

Palmqvist K, Campbell D, Ekblad A, Johansson H (1998) Photosynthetic capacity in relation to nitrogen content and its partitioning in lichens with different photobionts. Plant Cell Environ 21:361–372

Purvis OW, Coppins BJ, Hawksworth DL, James PW, Moore DM (1992) The lichen flora of Great Britain and Ireland. Natural History Museum Publications, London

Rai AN (1988) Nitrogen metabolism. In: Galun M (ed) CRC handbook of lichenology, vol 1. CRC, Boca Raton, Fla, pp 201–237

Raven JA (1992) Energy and nutrient acquisition by autotrophic symbioses and their asymbiotic ancestors. Symbiosis 14:33–60

Raven JA, Johnston AM, Handley LL, McInroy SG (1990) Transport and assimilation of inorganic carbon by *Lichina pygmea* under emersed and submersed conditions. New Phytol 114: 407–417

Reich PB, Walters MB, Ellsworth DS, Vose JM, Volin JC, Gresham C, Bowman WD (1998) Relationships of leaf dark respiration to leaf nitrogen, specific leaf area and leaf lifespan: a test across biomes and functional groups. Oecologia 114:471–482

Reich PB, Ellsworth DS, Walters MB, Vose JM, Gresham C, Volin JC, Bowman WD (1999) Generality of leaf trait relationships: a test across six biomes. Ecology 80:1955–1969

Richardson DHS (1999) War in the world of lichens: parasitism and symbiosis as exemplified by lichens and lichenicolous fungi. Mycol Res 6:641–650

Sancho LG, Valladares F, Schroeter B, Kappen L (2000) Ecophysiology of Antarctic versus temperate populations of a bipolar lichen: the key role of the photosynthetic partner. In: Davison W, Williams CH, Broady P (eds) Antarctic ecosystems: models for wider ecological understanding. New Zealand Natural Sciences Publications, Christchurch

Schulze ED, Chapin FSI (1987) Plant specialization to environments of different resource availability. In: Schulze ED, Zwölfer H (eds) Potentials and limitations of ecosystem analysis. Springer, Berlin Heidelberg New York, pp 120–148

Sundberg B, Campbell D, Palmqvist K (1997) Predicting CO_2 gain and photosynthetic light acclimation from fluorescence yield and quenching in cyanolichens. Planta 201:138–145

Sundberg B, Ekblad A, Näsholm T, Palmqvist K (1999) Lichen respiration in relation to active time, nitrogen and ergosterol concentrations. Funct Ecol 13:119–125

Sundberg B, Näsholm T, Palmqvist K (2001) The effect of nitrogen on growth and key thallus components in the two tripartite lichens, *Nephroma arcticum* and *Peltigera aphthosa*. Plant Cell Environ 24:517–527

Tehler A (1996) Systematics, phylogeny and classification. In: Nash TH III (ed) Lichen biology. Cambridge University Press, Cambridge, pp 217–239

Tretiach M, Carpanelli A (1992) Chlorophyll content and morphology as factors influencing the photosynthetic rate of *Parmelia caperata*. Lichenologist 24:81–90

Tretiach M, Pecchiari M (1995) Gas exchange rates and chlorophyll content of epi- and endolithic lichens from the Trieste Karst (NE Italy) New Phytol 130:585–592

Tschermak-Woess E (1988) The algal partner. In: Galun M (ed) CRC handbook of lichenology, vol 1. CRC, Boca Raton, Fla, pp 39–94

Valladares F, Sancho LG (2000) The relevance of nutrient availability for lichen productivity in the Maritime Antarctic. Bibl Lichenol 75:189–199

Valladares F, Sancho LG, Ascaso C (1996) Functional analysis of the intrathalline and intracellular chlorophyll concentrations in the lichen family *Umbilicariaceae*. Ann Bot 78:471–477

Weete JD (1973) Sterols of the fungi, distribution and biosynthesis. Phytochemistry 1:1843–1864

Wellburn AR (1994) The spectral determination of chlorophylls *a* and *b*, as well as total carotenoids, using various solvents with spectrophotometers of different resolutions. J Plant Physiol 144:307–313

Zotz G, Büdel B, Meyer A, Zellner H, Lange OL (1998) In situ studies of water relations and CO_2 exchange of the tropical macrolichen *Sticta tomentosa*. New Phytol 139:525–535